Journal of Hazardous Materials 172 (2009) 700–706

Contents lists available at ScienceDirect

Journal of Hazardous Materials

journal homepage: www.elsevier.com/locate/jhazmat

Effect of temperature on the formation of macroporous ZnO bundles and its application in photocatalysis

M. Muruganandham, I.S. Chen, J.J. Wu*

Department of Environmental Engineering and Science, Feng Chia University, Taichung 407, Taiwan

ARTICLE INFO

Article history:
Received 16 April 2009
Received in revised form 13 July 2009
Accepted 14 July 2009
Available online 22 July 2009

Keywords:
ZnO
Bundles
Photocatalyst
Methylene blue

ABSTRACT

In this article, the effects of temperature on the formation of macroporous zinc oxide bundles and its photocatalytic activity under a variety of experimental conditions were reported. Thermal decomposition of zinc oxalate dihydrate yields hexagonal wurtzite-type ZnO bundles. Increased the decomposition temperatures resulted in decreased time required for bundle formation, with a corresponding increase in nanoparticles agglomeration. ZnO bundle formation was facilitated up to 200 °C after complete decomposition of zinc oxalate into ZnO at 400 °C in 15 min. However, low temperature (such as 100 °C) was not facilitated nanobundle formation, suggesting the importance of temperature on ZnO bundles formation. In addition, nitrogen adsorption experiments confirmed the presence of macroporous structure in the bundles. The photocatalytic decolorization and adsorption of methylene blue dye (MB) on ZnO bundles were investigated under UV light irradiation. The adsorption and decolorization efficiency of macroporous bundles were higher than the fused bundles. In conclusion, ZnO bundles are efficient and easily recyclable photocatalyst.

© 2009 Elsevier B.V. All rights reserved.

1. Introduction

Zinc oxide is a well-known wurtzite type wide-band gap semiconductor and currently gained attention because of its electronic properties. Recently, the study of one-dimensional (1D) nanostructural ZnO has attracted much interest owing to its low cost, unique electrical, optoelectronic and luminescent properties with many potential applications [1–5]. The synthesis and application of new ZnO nanostructures is on the cutting edge of today's research in nanotechnology. Such attempts in nanomaterial growth must be improved from naturally occurring processes in order to be scalable for their practical applications.

Photocatalytic processes in polluted air and water can degrade the concentration of contaminants through the use of UV-irradiated inorganic oxides. In recent years, novel heterogeneous metal oxide semiconductor materials, for example, TiO_2 and ZnO, were developed, which attracted considerable attention due to their photocatalytic ability to degrade various environmental pollutants [6–10]. ZnO is a most effective process, like TiO_2, in photocatalytic decolorization under UV irradiation. Certain studies have confirmed that ZnO exhibits a better efficiency than TiO_2 in photocatalytic decolorization of select dyes even in aqueous solutions [11–13]. Other advantages of ZnO application were reported an absorption capacity with larger fractions of solar spectrum compared to TiO_2 [14].

Synthetic dyes are major industrial pollutants as a water contaminant [15]. Textile wastewater frequently introduces intensive color and toxicity residues into aquatic systems. Due to the complex aromatic structures and stability of these dyes, conventional biological treatment methods are at times ineffective as a pollutant degrader [16,17]. In many applications, ZnO was used to form fine powder particulates suspended in water. In spite of the simplicity of this technique, it is still necessary to recover the ZnO powders after photocatalytic water treatment. Researchers have used other methods to immobilize ZnO powders on a supporting material while searching for a new, easily recoverable photocatalyst process to offset the cost of recovery operations, and possible powder loss [18,19]. Earlier, we reported the fabrication of easily recyclable, wurtzite ZnO bundles and their catalytic activity in catalytic ozonation processes using 2-ethoxy ethyl acetate (2-EEA) as a model pollutant [1].

ZnO bundle synthesis under optimum experimental condition is necessary for large scale production and for energy saving purposes. Since we previously reported that the decomposition temperature played a crucial role in the formation of bundles, the practical effects of temperature on bundles formation needed further investigation. Although zinc oxalate was used as a starting material for the preparation of ZnO, no research results were available for ZnO bundle fabrication [20–22]. The aim of the present investigation was to study the ZnO bundle formation under a variety of experimental conditions, including adsorption and photocatalytic efficiency rates

* Corresponding author. Tel.: +886 4 24517250x5206; fax: +886 4 24517686.
E-mail address: jjwu@fcu.edu.tw (J.J. Wu).

0304-3894/$ – see front matter © 2009 Elsevier B.V. All rights reserved.
doi:10.1016/j.jhazmat.2009.07.053

using MB as a model pollutant under UV light irradiation. MB dye is not regarded as an acutely toxic component, but it has various harmful effects. Acute exposure to MB will cause increased heart rate, vomiting, shock, Heinz body formation, cyanosis, jaundice and quadriplegia and tissue necrosis in humans. Although MB is frequently seen in some medical uses in large quantities, it can also be widely used in coloring paper, dyeing cottons, wools, coating for paper stocks, etc.

2. Materials and methods

2.1. Chemicals

Methylene blue dye was obtained from Merck chemical company, Germany. Oxalic acid (anhydrous) (99%) and zinc nitrate hexa hydrate (99%) were purchased from SHOWA Chemical Co., Japan.

2.2. Preparation of zinc oxalate dihydrate

Aqueous solutions of equal volume of 0.4 M zinc nitrate hexa hydrate and of 0.6 M anhydrous oxalic acid in deionized water (Milli q-Plus, resistance = 18.2 MΩ) were brought to their boiling points and the former was added rapidly to the latter; the mixture was stirred often as it cooled down to room temperature. The precipitate is rather fine and uniform in dimension. The crystals were washed several times with distilled water, air-dried for over night, and dried 100 °C for 3 h. The sample was kept for further analysis in polyethylene cover.

2.3. Synthesis of ZnO bundles

About 1 g of zinc oxalate dihydrate was taken in a porcelain dish and kept inside the muffle furnace. The furnace was heated at the rate of 20 °C/min to reach the desired decomposition temperature. After desired time, the furnace was allowed to cool down automatically to room temperature. The synthesized ZnO bundle was collected and used for further analysis.

2.4. Photocatalytic reactor

The photocatalytic decomposition experiments were studied in an immersion type photoreactor which was assembled in our laboratory as shown in Fig. 1. This module consists of a double-walled glass vessel with its outer circulation space connected to a water bath for maintaining desired temperatures. Open borosilicate glass tubes of 200 ml capacity, with a 30 cm height and a 6 cm diameter, were used as reaction vessels. Required quantities of dye solution with catalyst were placed in the inner reactor as a decomposition experiment. In the center of cylindrical reactor, a lamp was placed inside the quartz tube (19 cm height, 2 cm diameter) in open-air conditions. A low-pressure mercury lamp (Pen-Ray, UVP Inc.) was used for irradiation purpose, which predominantly emits sole wavelength at 254 nm and has an intensity of 5.5 mW/cm^2 measured by UVX radiometer, UVP Inc. The temperature of the experimental solution was maintained at 25 °C by circulating water during the experiments. The aforementioned apparatus was placed in a magnetic stirrer for complete mixing of the catalyst with dye solution. In all cases, 50 ml of the MB dye solution (100 mg/l) containing appropriate quantity of the ZnO was used. The suspension was stirred for 30 min in the dark for the attainment of adsorption equilibrium. At specific time intervals, 4 ml of the sample was withdrawn and centrifuged to separate the catalyst. One milliliter of the centrifugate was diluted to 25 ml and its absorbance at 665 nm was measured. The maximum absorbance intensity at the wavelength of 665 nm was experimentally determined using a spectrophotometer (Spectronics, Genesys 5, USA) and it is used to monitor the decolorization of methylene blue (C.I. number 52015, molecular formula = $C_{16}H_{18}N_3ClS{\cdot}H_2O$, molecular weight = 355.89). The calibration curve obtained using solutions of known concentrations of the studied MB and was linear with a high correlation coefficient (R^2) 0.999. From this calibration curve, the initial and final concentration of MB was calculated as necessary.

2.5. Adsorption of MB on ZnO bundles

All adsorption experiments were carried out using a 5 mg/l of MB with 1 g/l of catalyst prepared at a neutral pH 6.9. Approximately 25 ml of dye solution with catalyst was collected in a polyethylene bottle and kept in a thermo-stated mechanical shaker for 24 h at 25 °C. After adsorption process, the catalyst was filtered and centrifuged from interfering concentration measurement. In order to avoid any photoreaction of ZnO on MB, the samples were kept in the dark for the entire period of the experiment.

2.6. Analytical methods

The X-ray diffraction (XRD) patterns were recorded using a MAX SCIENCE MXP3 diffractometer and Cu Kα radiation and 2θ scanned angle from 25° to 80° at the scanning rate of 2° per min. The surface area, pore size and pore volume of the ZnO bundles were mea-

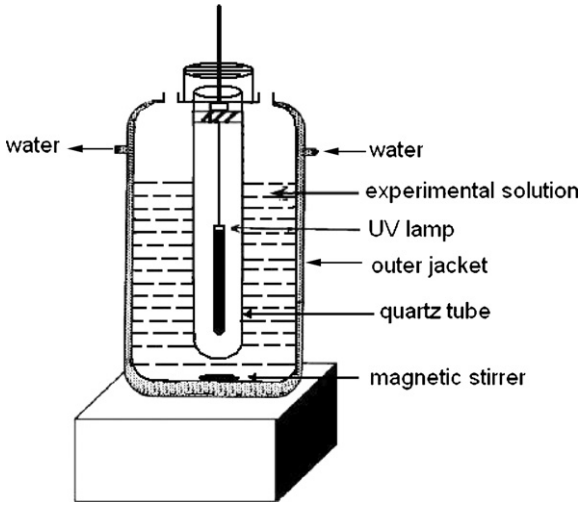

Fig. 1. Schematic diagram of photocatalytic reactor under UV light irradiation.

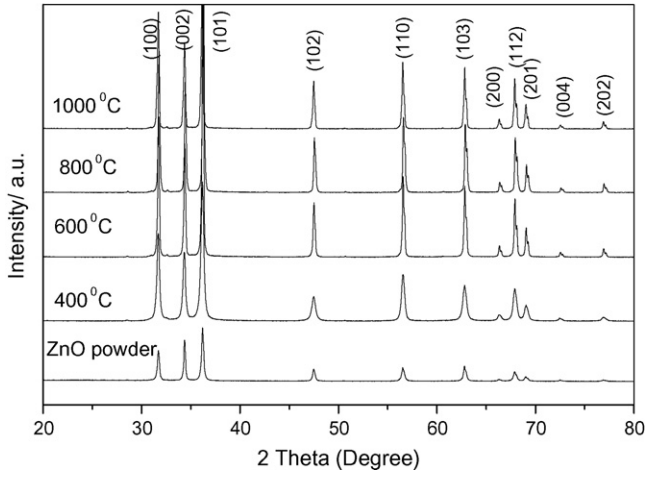

Fig. 2. XRD of ZnO powder and bundles formed at various decomposition temperatures.

Table 1
Surface analysis of ZnO bundles formed at various temperatures.

Sample no.	BET surface area (m^2/g)	Single point total pore volume (cm^2/g)	Adsorption average pore width (4V/A by BET) (Å)
1	11.9	0.37	125.9
2	1.2	0.001	65.6
3	1.0	0.001	50.7
4	23.9	0.121	202.4
5	18.8	0.097	207.3

[1] Bundles formed in 12 h at [2] 400 °C, [3] 600 °C, [3] 800 °C and after complete decomposition of the starting material at 400 °C in 15 min and then calcination at [4] 300 °C in 12 h, [5] 200 °C in 12 h.

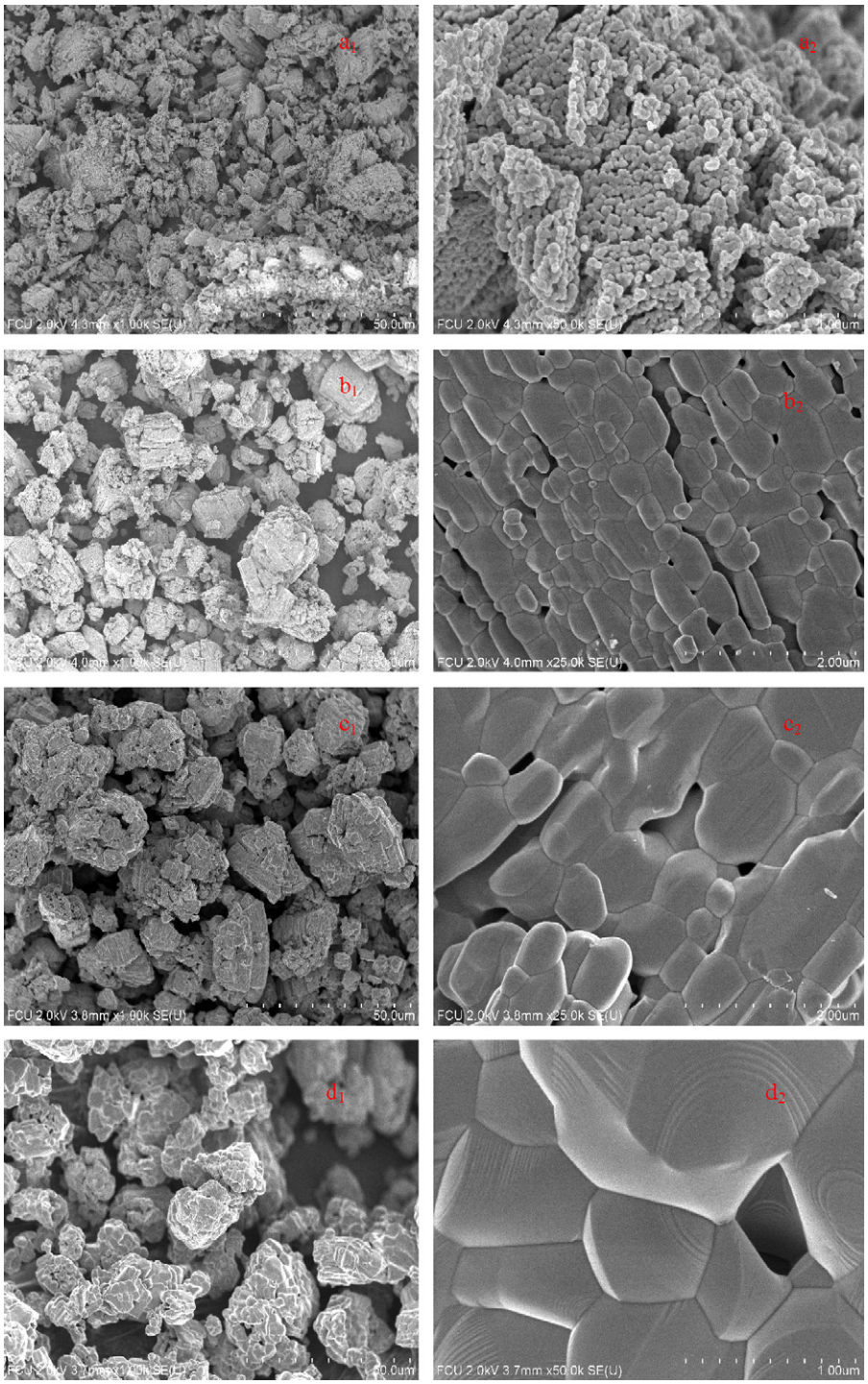

Fig. 3. FE-SEM pictures of ZnO formed after 12 h at (A) 400 °C ($a_1 \times 1k$, $a_2 \times 50k$), (B) 600 °C ($b_1 \times 1k$, $b_2 \times 25k$), (C) 800 °C ($c_1 \times 1k$, $c_2 \times 25k$), (D) 1000 °C ($d_1 \times 1k$, $d_2 \times 50k$).

sured by nitrogen adsorption at 77 K using an accelerated surface area and porosity apparatus (ASAP 2010, Micromeritics). Prior to analysis, 1–2 g of powder was degassed at 473 K for 2 h. High resolution transmission electron microscope (HR-TEM) images were recorded using a JEOL JEML-2010 high resolution transmission electron microscope. Samples for HR-TEM were prepared by ultrasonically dispersing the ZnO into ethanol, then a drop of this suspension placed onto a copper grid and air dried. The working voltage of TEM was 200 kV. The morphology of the catalyst was examined using a Hitachi S-4800 cold field emission scanning electron microscope (FE-SEM). Before FE-SEM measurements, the samples were mounted on a carbon platform then placed in the scanning electron microscope for subsequent analysis at various magnifications.

3. Results and discussion

3.1. Effect of temperature on the ZnO bundles fabrication

In our earlier reports we found that the thermal decomposition of zinc oxalate dihydrate at 400 °C in 12 h would result in ZnO bundles. The current study focused on ZnO bundles formation at various temperatures using similar analytical techniques. XRD results of ZnO bundle synthesized at 400, 600, 800 and 1000 °C are presented in Fig. 2. It is noted that all XRD peaks of bundles are well matched with standard ZnO powder. The XRD patterns of ZnO formed at four different temperatures were quit similar and good agreements with hexagonal standard ZnO (JCPDS Card No. 89-0511). The crystallographic phase of these ZnO bundles belongs to the wurtzite-type ZnO (SG: *P*63*mc*). Characteristic peaks of ZnO at 31.68, 34.36, 36.18 and 56.56, corresponds to (1 0 0), (0 0 2), (1 0 1) and (1 1 0) diffraction peaks of wurtzite ZnO, indicating that the ZnO shell possess a hexagonal crystal structure. The relatively high intensity of the (1 0 1) peak is indicative of anisotropic growth and implies a preferred orientation of the crystallites. It is interesting to note the morphology of ZnO bundles formed at various temperatures as shown in Fig. 3a shows that the ZnO bundles formed at 400 °C, which are consist of nanoparticles with size ranging from 10 to 70 nm and no nanoparticles aggregation noted. However, nanoparticles were agglomerated at higher temperature and the degree of agglomeration increased with increasing temperatures from 400 to 1000 °C as shown in Fig. 3b–d. To understand surface properties of ZnO bundles formed at various temperatures, the nitrogen-adsorption experiments were performed and the results are presented in Table 1. As expected, increasing the decomposition temperature, the surface area, pore size, and pore volume of the bundles were decreased due to agglomeration of nanoparticles. After complete decomposition of zinc oxalate into ZnO at 400 °C in

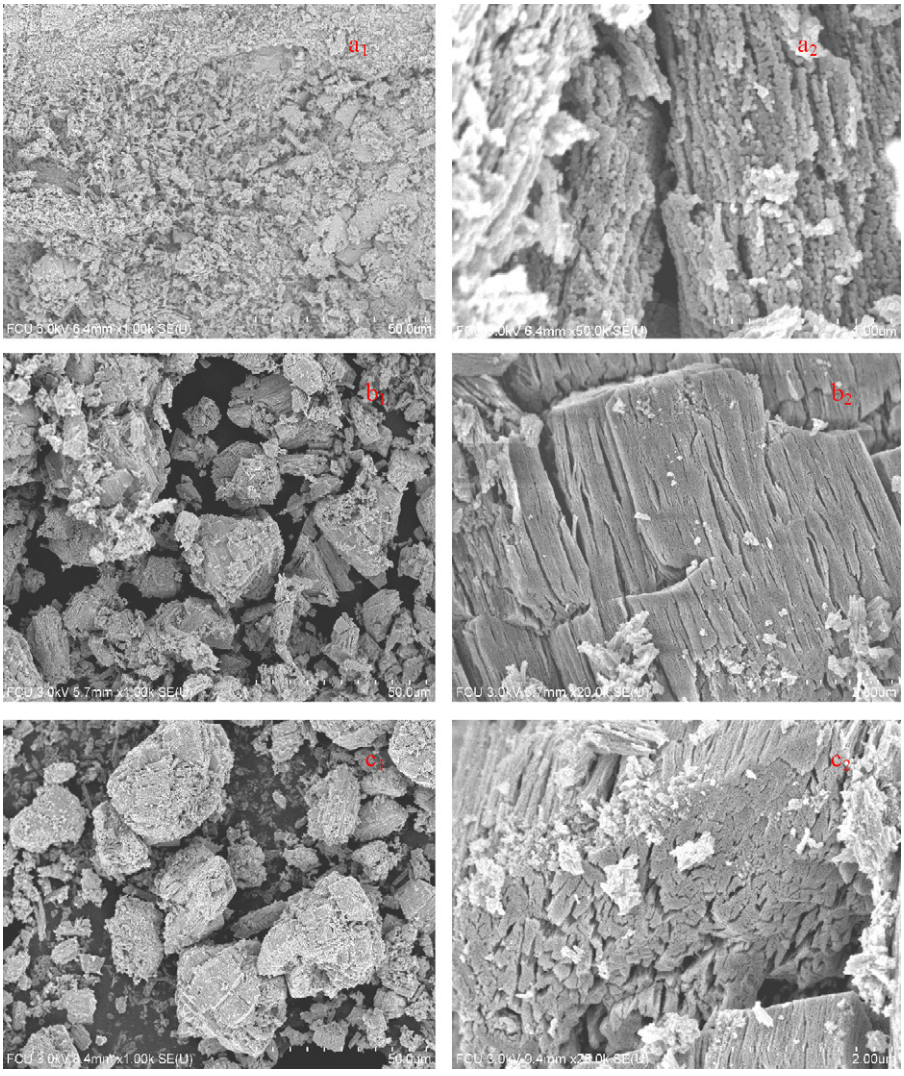

Fig. 4. FE-SEM pictures of ZnO formed after decomposition at 400 °C in 15 min followed by calcined at 12 h at (A) 100 °C ($a_1 \times 1k$, $a_2 \times 50k$), (B) 200 °C ($b_1 \times 1k$, $b_2 \times 20k$), (C) 300 °C ($c_1 \times 1k$, $c_2 \times 20k$).

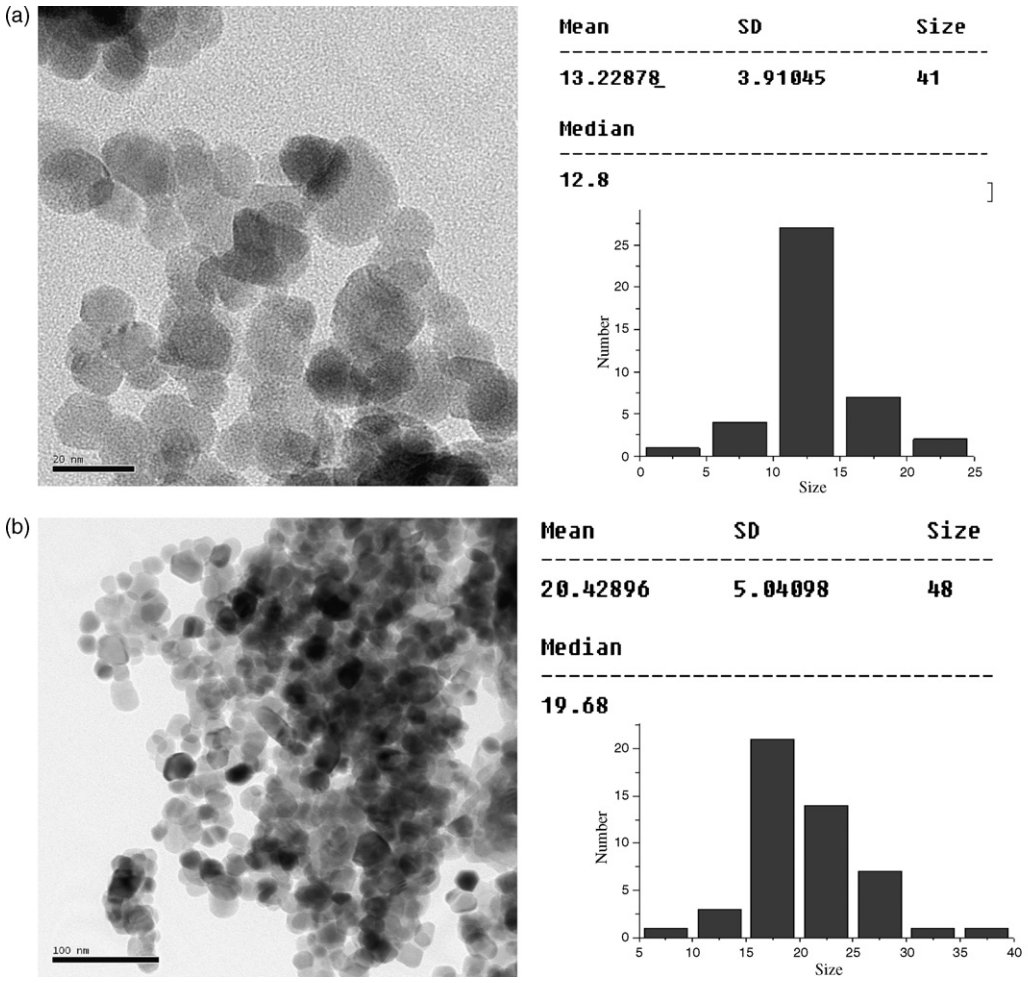

Fig. 5. HR-TEM particle size analysis of ZnO bundles formed at (a) 200 and (b) 300 °C.

15 min and followed by calcinations at 100, 200, and 300 °C over 12 h was studied and the results are present in Fig. 4. Bundles were formed at temperatures of 200 and 300 °C with the particle size about 1–25 nm with an average of 13.2 and 5–40 nm with an average of 20.42 nm were noted respectively, as shown in Fig. 5a and b. However, calcinations at 100 °C was not facilitated effective bundle formation, which demonstrates the importance of calcination temperatures for bundles formation. These results suggest that particle size can be controlled by the calcination temperature. However, no nanoparticles were noted at higher temperature and therefore we do not present the particle size at higher decomposition temperature. The particle size in the bundles depends on calcination temperature. Surface analysis of ZnO bundles formed at various temperatures is presented in Table 1. Nitrogen adsorption isotherm results confirmed the presence of macrospores with an average pore size around 20 nm and pore volume noted at about 0.1 cm^3/g. These macrospores formed in-between the nanoparticles and adjacent chains in the bundles. The surface area, pore volume, and pore size of the bundles increased with decreased calcination temperatures due to particle agglomerization. Bundles could be produced in a short time when the synthesis temperatures increased over 400 °C. Bundles were also formed within 1 h and 5 min at 450 and 600 °C as shown in Fig. 6. Although bundles are formed in a short time, nanoparticles size and agglomeration of particles were increased when compared to bundles formed at lower temperature. ZnO bundle formation was also tested by using various zinc oxalate dihydrate prepared at different methods which yielded similar ZnO bundles. These results confirmed that the bundle formation could not be affected by the preparation method of zinc oxalate.

3.2. Adsorption of MB on bundles

Adsorption experiments were conducted to understand MB adsorption on various ZnO bundles formed at different temperatures. Generally, adsorption of dye on the catalyst surface depends on charge of dye molecules and surface charge of the catalysts. Since MB is a cationic dye, it would behave as a cationic molecule at pH 6.8 (natural pH). The point of zero charge position depends on the acid-alkali character of surface hydroxyl groups. For zinc oxide, the value of this parameter is in a wide range from 6.9 to 9.8 [22]. Therefore, the ZnO surface is positively charged in pH < 6.9 whereas it is negatively charged under alkaline conditions (pH > 9.5). At pH 6.8, both surfaces of zinc oxide and MB dye behave as positively charged molecules. Therefore, the adsorption of dye on the bundles would be relatively limited. The adsorption results are presented in Fig. 7. MB adsorption slightly decreased when the bundles synthesis temperature increased, due to the decrease of the surface area of catalyst as seen in Table 1. Higher adsorption of MB was noted on noncoalescent nanoparticles formed at the early stage of decomposition in the presence of polar surfaces [1]. Polar surfaces favors higher adsorption rates due to electrostatic attraction between negatively charged surface terminations with positively charged dye.

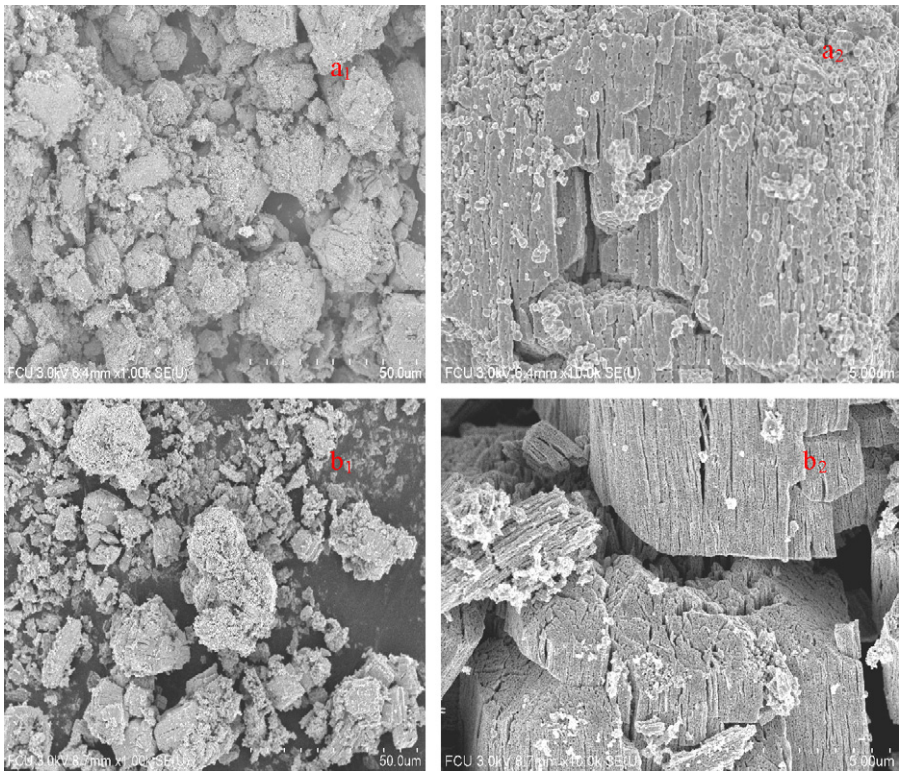

Fig. 6. FE-SEM pictures of ZnO formed at (A) 600 °C in 5 min ($a_1 \times 1k$, $a_2 \times 10k$), (B) 450 °C in 1 h ($b1 \times 1k$, $b_2 \times 10k$).

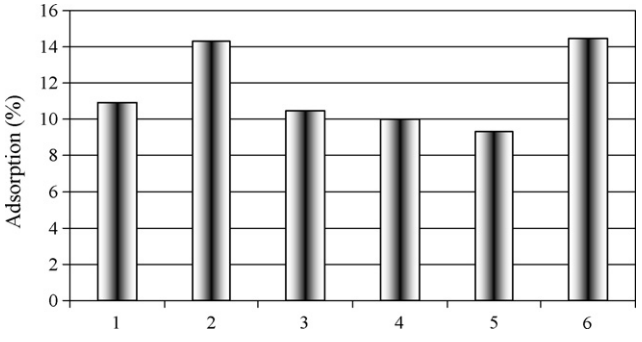

Fig. 7. Adsorption of MB dye on ZnO bundles formed at various experimental conditions. [MB] = 5 mg/l, pH = 6.8, [catalyst] = 25 mg, temperature = 25 °C. [1] Calcination at 400 °C in 12 h, [2] after complete decomposition of the starting material at 400 °C in 15 min, [3] calcination at 600 °C in 12 h, [4] calcination at 800 °C in 12 h and after complete decomposition of the starting material at 400 °C in 15 min and then calcination at [5] 200 °C in 12 h, [6] 300 °C in 12 h.

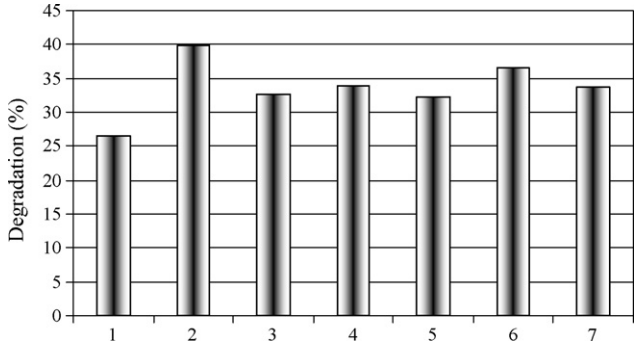

Fig. 8. Photocatalytic decolorization of MB using ZnO bundles synthesized at various experimental conditions. [MB] = 100 mg/l, pH = 5.1, [catalyst] = 50 mg, temperature = 25 °C. [1] Photo bleaching of dye by UV light in the absence of photocatalyst, [2] calcination at 400 °C in 12 h, [3] after complete decomposition of the starting material in 15 min, [4] calcination at 600 °C in 12 h, [5] calcination at 800 °C in 12 h and after complete decomposition of the starting material at 400 °C in 15 min and then calcination at [6] 200 °C in 12 h, [7] 300 °C in 12 h.

3.3. Photocatalytic decolorization of MB dye

All photocatalytic decomposition experiments were carried out under similar experimental conditions using 100 mg/l of dye solution with ZnO bundles catalysts. No buffer was added into the reaction mixture, avoiding the addition of anions that may have interfered with processes occurring on catalytic surfaces [23]. For this reason, all experiments were conducted at a neutral pH (5.1). Before UV irradiation, aqueous dye solution containing photocatalyst were stirred magnetically in the dark for 30 min to achieve adsorption/desorption equilibrium among dye, photocatalyst, and dissolved oxygen and the results are shown in Fig. 8. Photolysis of MB in the presence of UV light was tested in the absence of catalysts. About 26.5% of decolorization was noted in 60 min. Additionally, about 39.7% of MB decolorization was observed in the presence of the catalyst, demonstrating the effectiveness of photocatalyst. It is worth noting that bundles formed at 400 °C resulted in higher photocatalytic activity than all other bundles prepared at various temperatures. This is due to the formation of well crystallized porous bundles. The combination of semiconductor and UV light generates highly reactive compounds, namely hydroxyl radicals which eventually degrade the pollutants, and the details of mechanism have been well documented in the literature [24]. The photocatalytic activity of bundles is different from adsorption properties, indicating that adsorption is not an important process for photocatalytic activity of ZnO bundles.

4. Conclusion

ZnO bundles fabrication by using thermal decomposition of zinc oxalate at various temperatures have been studied. XRD results

showed that well crystallized, hexagonal wurtzite phase ZnO bundles were formed at all decomposition temperature. Increasing the decomposition temperature over 400 °C caused particle agglomeration resulting in fused bundles at high temperatures. The particle size in the ZnO bundles can be controlled by varying decomposition temperatures of the starting material. About 13.2 and 20.4 nm of average particle size was noted at 200 and 300 °C, respectively. ZnO bundles formed in a short time when decomposition temperatures increased over 400 °C. ZnO bundles surface property such as surface area, pore volume and pore size, depends on synthesis temperatures. Adsorption and photocatalytic decomposition results noted a relationship between surface properties of the bundles. Higher methylene blue adsorption and photocatalytic decolorization were noted on bundles formed at 400 and 300 °C, respectively compared to bundles formed at other temperatures.

Acknowledgement

The authors wish to thank the financial support from the National Science Council in Taiwan under the project contract number of NSC-97-2221-E-035-033.

References

[1] M. Muruganandham, J.J. Wu, Synthesis, characterization and catalytic activity of easily recyclable zinc oxide bundles, Appl. Catal. B: Environ. 80 (2008) 32–41.
[2] X.D. Wang, C.J. Summers, Z.L. Wang, Large-scale hexagonal-patterned growth of aligned ZnO nanorods for nano-optoelectronics and nanosensor arrays, Nano Lett. 4 (2004) 423–426.
[3] C.Y. Jiang, X.W. Sun, G.Q. Lo, D.L. Kwong, Improved dye-sensitized solar cells with a ZnO-nanoflower photoanode, Appl. Phys. Lett. 90 (2007) 263501.
[4] J.H. He, S.T. Ho, T.B. Wu, L.J. Chen, Z.L. Wang, Electrical and photoelectrical performances of nano-photodiode based on ZnO nanowires, Chem. Phys. Lett. 435 (2007) 119–122.
[5] E. Yassıtepe, H.C. Yatmaz, C. Ozturk, K. Ozturk, C. Duran, Photocatalytic efficiency of ZnO plates in decolourization of azo dye solutions, J. Photochem. Photobiol. A: Chem. 198 (2008) 1–6.
[6] V. Houskova, V. Stengl, S. Bakardjievaa, N. Murafa, Photoactive materials prepared by homogeneous hydrolysis with thioacetamide: part 2-TiO_2/ZnO nanocomposites, J. Phys. Chem. Sol. 69 (2008) 1623–1631.
[7] N. Daneshvar, S. Aber, M.S. Seyed, A.R. Dorraji, M.H. Khataee, Rasoulifard, Photocatalytic decolourization of the insecticide diazinon in the presence of prepared nanocrystalline ZnO powders under irradiation of UV-C light, Sep. Purif. Technol. 58 (2007) 91–98.
[8] M. Mrowetz, E. Selli, Photocatalytic decolourization of formic and benzoic acids and hydrogen peroxide evolution in TiO_2 and ZnO water suspensions, J. Photochem. Photobiol. A: Chem. 180 (2006) 15–22.
[9] C. Hariharan, Photocatalytic decolourization of organic contaminants in water by ZnO nanoparticles: revisited, Appl. Catal. A: Gen. 304 (2006) 55–61.
[10] H.C. Yatmaz, A. Akyol, M. Bayramoglu, Kinetics of the photocatalytic decolorization of an azo reactive dye in aqueous ZnO suspensions, Ind. Eng. Chem. Res. 43 (2004) 6035–6039.
[11] C.A.K. Gouvea, F. Wypych, S.G. Moraes, N. Duran, N. Nagata, P.P. Zamora, Semiconductor-assisted photocatalytic decolourization of reactive dyes in aqueous solution, Chemosphere 40 (2000) 433–440.
[12] S.K. Kansal, M. Singh, D. Sud, Studies on photodecolourization of two commercial dyes in aqueous phase using different photocatalysts, J. Hazard. Mater. 141 (2007) 581–590.
[13] N. Sobana, M. Swaminathan, The effect of operational parameters on the photocatalytic decolourization of acid red 18 by ZnO, Sep. Purif. Technol. 56 (2007) 101–107.
[14] S. Chakrabarti, B.K. Dutta, Photocatalytic decolourization of model textile dyes in wastewater using ZnO as semiconductor catalyst, J. Hazard. Mater. 112 (2004) 269–278.
[15] D.H. Brown, H.R. Hitz, L. Schafer, The assessment of the possible inhibitory effect of dyestuffs on aerobic waste-water bacteria experience with a screening test, Chemosphere 10 (1981) 245–261.
[16] U. Pagga, D. Brown, The decolourization of dyestuffs: part II. Behaviour of dyestuffs in aerobic biodecolourization tests, Chemosphere 15 (1986) 479–491.
[17] N.H. Ince, D.T. Gonenc, Treatability of a textile azo dye by UV/H_2O_2, Environ. Technol. 18 (1997) 179–185.
[18] X. Meng, B. Lin, Z. Fu, Influence of CH_3COO^- on the room temperature photoluminescence of ZnO films prepared by CVD, J. Lumin. 126 (2007) 203–206.
[19] Q. Zhang, W. Fan, L. Gao, Anatase TiO_2 nanoparticles immobilized on ZnO tetrapods as a highly efficient and easily recyclable photocatalyst, Appl. Catal. B: Environ. 76 (2007) 168–173.
[20] L. Yang, G. Wang, C. Tang, H. Wang, L. Zhang, Synthesis and photoluminescence of corn-like ZnO nanostructures under solvothermal-assisted heat treatment, Chem. Phys. Lett. 409 (2005) 337–341.
[21] Z. Jia, L. Yue, Y. Zheng, Z. Xu, Rod-like zinc oxide constructed by nanoparticles: synthesis, characterization and optical properties, Mater. Chem. Phys. 107 (2008) 137–141.
[22] Kosmulski, Chemical Properties of Material Surfaces, Surfactant Sci. Series, v. 102, M. Dekker Inc., 2001.
[23] W. Baran, A. Makowski, W. Wardas, The influence of inorganic ions on the photocatalytic decolourization of Orange II in aqueous solutions, Eng. Prot. Environ. 6 (2003) 75–85.
[24] M.R. Hoffmann, S.T. Martin, W. Choi, D.W. Bahnemann, Environmental applications of semiconductor photocatalysis, Chem. Rev. 95 (1995) 69–96.